

## MICRO-THERMAL FIELD-FLOW FRACTIONATION OF COLLOIDAL PARTICLES: EFFECT OF TEMPERATURE ON RETENTION AND RELAXATION PROCESSES

Josef JANČA

*Université de La Rochelle, Pôle Sciences et Technologie, Avenue Michel Crépeau,  
17042 La Rochelle Cedex 01, France; e-mail: jjanca@univ-lr.fr*

Received September 27, 2002

Accepted November 14, 2002

An important decrease in the heat flux across the micro-thermal field-flow fractionation (micro-TFFF) channel compared with the standard size channel allowed to control independently the temperatures of the cold and hot walls and to study the behaviour of colloidal particles within an extended temperature range. The only limitation was imposed by the freezing and boiling points of the carrier liquid. The retention and the relaxation processes were found to be influenced by temperature. A decrease in the viscosity of the carrier liquid with increasing temperature results in an increase in the diffusion coefficient of the retained species. Consequently, the relaxation processes associated with the establishment of the steady-state concentration distribution are accelerated, the time to reach the steady state decreases with increasing temperature, and the retention ratio of moderately retained particles decreases to reach a minimum value. The fractograms of colloidal samples of narrow particle size distribution (PSD) obtained at lowest temperatures can exhibit two peaks; the first corresponding to the unrelaxed particles eluted even at higher than the average velocity of the carrier liquid and the second one corresponding to the particles retained less compared with the zone eluted at a steady state from the very beginning. The further increase in temperature above that at which the retention ratio reaches the mentioned minimum produces inversion of the retention ratio, *i.e.* its increase. The peak corresponding to the unrelaxed part of the particles progressively disappears with increasing temperature. If the flow of the carrier liquid is stopped immediately after the injection of the sample for a time to reach a steady-state concentration distribution of the particles across the channel and restarted after that period, the retention ratio does not exhibit a pronounced minimum. On the other hand, the width of the zone generally decreases with increasing temperature but less if the stop-flow procedure is applied. These findings confirm that the retention ratio is influenced by temperature in agreement with the theoretical prediction. A practical conclusion is that higher resolution and reduced time of the separation can be achieved at higher temperatures of the accumulation wall. The micro-TFFF thus becomes a highly competitive method of separation and determination of the PSD of colloidal particles.

**Keywords:** Micro-thermal field-flow fractionation; Colloidal particles; Relaxation phenomena; Effect of temperature.

Micro-thermal field-flow fractionation (micro-TFFF) is a brand new technique proposed and developed recently<sup>1-3</sup>. It has been applied to separations of polymers<sup>1,2</sup> and colloidal particles<sup>3</sup>. Although the temperature of the accumulation wall is an important factor, besides the temperature drop  $\Delta T$  influencing the retention, only few papers<sup>4-6</sup> dealt with the effect of the cold wall temperature on the retention of lipophilic polymers within a limited range of molar masses and cold wall temperatures. The reason for this surprisingly low interest concerning the effect of the cold wall temperature was probably due to technical problems related with the temperature control. The high heat flux between the hot and cold wall (with an electric power of the order of kilowatts) in standard size TFFF channels makes difficult any temperature control of both walls due to the difficulty to evacuate the high heat flux from the cold wall at a chosen temperature. The temperature of the tap water used frequently to cool the cold wall cannot obviously be chosen. Thus the only controlled parameter was the temperature drop  $\Delta T$ . On the other hand, the micro-TFFF provides the possibility to control any temperature of the cold or hot walls within a very large range of the temperature drops  $\Delta T$  with the only restriction imposed by the freezing and boiling points of the carrier liquid.

We have already studied<sup>2</sup> the effect of the cold wall temperature under the conditions of the micro-TFFF applied to the fractionation of polymers of ultra-high molar masses (UHMM) by working at as low cold wall temperature as 275 K. It has been found<sup>2</sup> that higher resolution and shorter time of the fractionation can be achieved at higher temperature of the cold wall in micro-TFFF carried out at constant  $\Delta T$ . The temperature dependence of the diffusion coefficient  $D$ , thermal diffusion coefficient  $D_T$ , viscosity of the carrier liquid  $\eta$  and, finally, of the relative viscosity of the polymer solution within the zone of the retained species influence not only the retention but also the dispersive processes. Complex relationships between the molecular characteristics of the polymers and the corresponding diffusion coefficients, the dependence of the viscosity of the carrier liquid on temperature, and the viscosity variation of the polymer solution with temperature reflecting the interactions between macromolecules and the solvent, are governed by empirical or semi-empirical rules, which make purely theoretical analysis impossible.

On the other hand, the colloidal particles can, in some cases, be considered as dilute suspensions of the hard spheres. Consequently, the theoretical prediction of their behaviour as a function of temperature under the conditions of the micro-TFFF can be easier. One objective of this study was then to analyze theoretically and to demonstrate experimentally the effect

of temperature of the accumulation wall on the retention and relaxation, and dispersion processes of the colloidal particles separated by the micro-TFFF.

In this context, it is necessary to mention a recent paper<sup>7</sup> describing the construction of a channel with the use of the non-metal materials of low thermal conductivity. In such a channel<sup>7</sup>, the high temperature difference of 46 K measured outside the channel must be established to obtain as low effective temperature drop as 4.8 K while a much higher temperature drop is necessary to fractionate small colloidal particles and macromolecules<sup>8,9</sup>. Consequently, it is not clear what is the advantage of such a channel compared with the micro-TFFF channel built up using metal materials<sup>1</sup>. The experimental plate heights  $H$  were calculated from the fractogram in Fig. 7 of ref.<sup>7</sup>, using the well-known relationship:

$$H = L \left( \frac{\sigma}{V_R} \right)^2, \quad (1)$$

where  $L$  is the length of the channel,  $V_R$  is the retention volume of the concerned solute, and  $\sigma$  is the standard deviation characterizing the width of the fractogram in the same volume units as  $V_R$ . The plate height calculated for the unretained solute in Fig. 7 of ref.<sup>7</sup> is  $H = 0.93$  cm. With respect to the elution time 31.2 s of this unretained solute and the given flow rate 1.25 ml/h, the only possible dimensions of the separation channel are  $27 \mu\text{m} \times 6 \text{ mm} \times 6.5 \text{ cm}$ . The linear velocity of the carrier liquid (calculated by dividing the volumetric flow rate by the cross-section of the channel) was then  $\langle v \rangle = 0.214$  cm/s. On the other hand, the plate height corresponding to the  $\langle v \rangle = 0.214$  cm/s taken from Fig. 5 of ref.<sup>7</sup> is roughly  $H = 1.2$  cm. The origin of the important difference compared with the above calculated  $H = 0.93$  cm is not clear but still its magnitude is not dramatic under the assumption that the legend in Fig. 5 of ref.<sup>7</sup> is correct (even if contradictory to the caption under this figure).

The problem is that the fractogram in Fig. 7 of ref.<sup>7</sup> is assumed to represent separation of two different size colloidal samples. As the void volume peak in Fig. 7 is very broad and indicates an important zone spreading due to the separation system, it is impossible to understand how two other peaks in Fig. 7 can correspond to the separation of two retained colloidal samples of different particle sizes. This assumption seems to be unjustified because both two peaks are substantially narrower than the void volume peak but such a result is theoretically impossible<sup>10,11</sup> and the known experi-

mental FFF data<sup>8,9</sup> generally confirmed the theory regardless of the fact that two theoretical approaches of the same principal author provide completely different results<sup>10,11</sup>, surprisingly not commented so far.

When neglecting the contribution of the longitudinal diffusion and of the extra-channel elements to the zone broadening, the approximate relationship<sup>10</sup> for the plate height  $H$  based on the theory of the zone broadening in FFF<sup>8,9</sup> combined with the well-known Stokes–Einstein relationship (given below) for the diffusion coefficient of a suspension of the hard spherical particles can be written as:

$$H = \frac{\chi w^2 \langle v \rangle}{D} = \frac{2R^3 w^2 \langle v \rangle \pi \eta r_p}{3k_B T}, \quad (2)$$

where  $R$  is the retention ratio defined below,  $w$  is the thickness of the channel,  $\langle v \rangle$  is the average linear velocity of the carrier liquid,  $r_p$  is the particle radius,  $k_B$  is Boltzmann constant,  $T$  is temperature, and  $\chi = 24\lambda^3$  where  $\lambda$  is the dimensionless parameter also defined below. A simple calculation with the use of Eq. (2) and of the experimental data given in ref.<sup>7</sup>, namely  $w = 27 \mu\text{m}$ ,  $\langle v \rangle = 0.214 \text{ cm/s}$ ,  $T = 297 \text{ K}$  (cold wall temperature),  $\eta = 0.0094 \text{ P}$  for water at 297 K, and the retention ratios  $R_1 = 0.441$ ,  $R_2 = 0.312$ , corresponding to the peaks of the retained particles 204 and 272 nm in Fig. 7 of ref.<sup>7</sup>, provides the plate heights  $H_{1,\text{theor}} = 0.654 \text{ cm}$  and  $H_{2,\text{theor}} = 0.309 \text{ cm}$ , respectively. On the other hand, the experimental plate heights values calculated from the fractogram in Fig. 7 of ref.<sup>7</sup> by using Eq. (1) are  $H_{1,\text{exp}} = 0.017 \text{ cm}$  and  $H_{2,\text{exp}} = 0.0021 \text{ cm}$ , respectively. The experimental dependence of the plate height on the linear velocity in Fig. 5 of ref.<sup>7</sup> shows clearly that the efficiency of the described separation system measured by the plate height is largely below the theoretical values. Consequently, by taking into account the theory, the retained peaks in Fig. 7 of ref.<sup>7</sup> should be at least 6.5× and 13× larger, respectively, and unresolved even if the PSD of both samples is completely neglected. As a result, it seems that the assumed separation in Fig. 7 of ref.<sup>7</sup> is an artifact.

Another goal of this study was then to prove that high performance separation of colloidal particles can be achieved in micro-TFFF channel provided its construction is optimized and the experiments are carried out correctly under the appropriate experimental conditions and interpreted accurately.

## THEORY

*Dependence of the Retention on Temperature*

The retention ratio in FFF is described by<sup>10</sup>:

$$R = 6\lambda[\coth(1/2\lambda) - 2\lambda] = V_0 / V_R, \quad (3)$$

where  $V_0$  is the elution volume of an unretained species which is equal to the void volume of the channel,  $V_R$  is the retention volume of a retained species, and  $\lambda$  is the retention parameter,  $\lambda = \ell/w$ , where  $\ell$  is a distance between the accumulation wall and the center of gravity of the concentration distribution of the retained species across the channel. Whenever the  $\lambda$  is small for highly retained species, Eq. (3) simplifies and becomes:

$$\lim_{\lambda \rightarrow 0} R = 6\lambda. \quad (4)$$

Equations (3) and (4) are rigorously valid only if the parabolic flow velocity profile is formed inside the channel under the isothermal conditions of isoviscous flow of the carrier liquid. Such a condition is not fulfilled in TFFF due to the viscosity variation with temperature across the channel. The retention ratio,  $R_{np}$ , which takes into account a non-parabolic flow velocity profile was described by Brimhall *et al.*<sup>5</sup> by a modified relationship:

$$R_{np} = 6\lambda\kappa(1 - R) + R, \quad (5)$$

where  $\kappa$  is a constant whose value is determined by the properties of the carrier liquid, the cold wall temperature and the field strength<sup>5</sup>, and  $R$  is the retention ratio under the conditions of the isoviscous flow. By substituting from Eq. (4) into Eq. (5) and by neglecting the term with  $\lambda$ , we obtain for highly retained species:

$$\lim_{\lambda \rightarrow 0} R_{np} = 6\lambda(1 + \kappa). \quad (6)$$

For highly retained species ( $\lambda \rightarrow 0$ ), the errors following from the approximate Eq. (6) do not exceed the level of experimental uncertainty of the  $\mu$ -TFFF data (roughly 1–2%).

The retention parameter  $\lambda$  is defined under the above mentioned conditions by<sup>5</sup>:

$$\lambda = \frac{1}{\left(\frac{\alpha_T}{T} + \gamma_T\right) \frac{dT}{dx} w}, \quad (7)$$

where  $\gamma_T$  is the coefficient of thermal expansion of the carrier liquid,  $dT/dx$  is temperature gradient across the channel, and  $\alpha_T$  is thermal diffusion factor defined by:

$$\alpha_T = \frac{D_T T}{D}. \quad (8)$$

Obviously, the transport coefficients  $D$  and  $D_T$  are also temperature-dependent and this dependence has a direct impact on Eq. (3)<sup>12</sup>. However, it has been concluded<sup>12</sup> that the errors introduced by neglecting the temperature dependence of the transport coefficients partly compensate errors due to the assumption of an isoviscous flow velocity profile. Whenever the retention is high enough ( $\lambda \rightarrow 0$ ), the resulting errors are negligible. As far as the thermodiffusion of the colloidal particles is still only a marginally understood phenomenon and with regard to the purpose of this work, the following approximations concerning the retention of colloidal particles in FFF are acceptable and justified by their mathematical simplicity and transparency.

The dependence of the diffusion coefficient  $D$  of the colloidal particles (considered hard spheres) on temperature is given by the above mentioned Stokes–Einstein relationship:

$$D = \frac{k_B T}{6\pi\eta r_p}. \quad (9)$$

The coefficient  $\gamma_T$  is negligible compared with the term  $\alpha_T/T$  in Eq. (7) and the temperature gradient  $dT/dx$  can be considered as constant whenever the temperature drop across the channel  $\Delta T$  is not very high. In such a case, the retention parameter  $\lambda$  can be written in a simplified form as:

$$\lambda = \frac{T}{\alpha_T \Delta T}. \quad (10)$$

We have not found in the literature relevant data concerning the temperature dependence of  $D_T$  of colloidal particles. The experimental findings<sup>5</sup> concerning the temperature dependence of  $D_T$  of flexible macromolecules in solution cannot be taken as reference because this dependence can be due to the variation of the size of macromolecular coils in solution and polymer-solvent interactions with temperature, which is certainly a different case compared with the hard spherical colloidal particles. On the other hand, the empirical relationships describing variation of the viscosity of the liquids are usually given either in the form of an exponential function such as:

$$\eta = a \exp\left(\frac{b}{T}\right) \quad (11)$$

or power series such as:

$$\frac{1}{\eta} = a_0 + a_1 T + a_2 T^2 + a_3 T^3, \quad (12)$$

where  $a$ ,  $b$  and  $a_i$  are the constants,  $i = 0, 1, 2, \dots$ . As a result, by combining Eqs (6), (8) to (10) and (12), we get:

$$\lim_{\lambda \rightarrow 0} R_{\text{np}} = (1 + \kappa) \frac{k_B T(a_0 + a_1 T + a_2 T^2 + a_3 T^3)}{\pi \Delta T D_T(T) r_p}. \quad (13)$$

Equation (13) shows that the temperature dependences of the thermal diffusion coefficient  $D_T(T)$  of colloidal particles and of the viscosity of the carrier liquid can be the crucial factors determining the casual variation of the retention ratio  $R$  with temperature.

### *Relaxation*

The establishment of the steady-state concentration distribution of the retained species after the injection is not immediate. If the flow of the carrier liquid is not stopped after the injection, the retained species migrate across the channel in the direction from the depletion to the accumulation wall (due to their interaction with the field) to reach their steady-state position and, simultaneously, along the channel due to the hydrodynamic flow. Consequently, a significant part of the retained species can move in the direction of the flow with the velocities corresponding to their current posi-

tions within the flow velocity profile, which are higher than the average velocity of the steady-state zone. If this relaxation period until the establishment of the steady-state zone is significant in comparison with the retention time, the resulting retention time is shorter and the zone is broader compared with a theoretical zone eluted under steady-state conditions from the very beginning. As a result, the resolution of the fractionated species is substantially deteriorated. In order to avoid this unfavourable situation, the flow of the carrier liquid can be stopped immediately after the sample injection for a period necessary to establish a quasi-steady-state concentration distribution across the channel and then restarted to carry out the fractionation under the optimum conditions.

The optimization of the stop-flow procedure was studied in detail both theoretically and experimentally for the sedimentation FFF of colloidal particles<sup>13</sup>. The relaxation time derived<sup>13</sup> on the basis of the accurate approach of Mason and Weaver<sup>14</sup> is:

$$t_{\varepsilon} = w^2 F(\lambda) / D, \quad (14)$$

where the function  $F(\lambda)$  is given by:

$$F(\lambda) = -\frac{1}{\pi^2 U(\lambda)} \ln \left\{ \frac{\pi^2 U(\lambda) \varepsilon}{4[1 + \cosh(1/2\lambda)]} \right\}, \quad (15)$$

where

$$U(\lambda) = 1 + 1 / (4\pi^2 \lambda^2). \quad (16)$$

The factor  $\varepsilon$  defines the relative deviation of the actually achieved concentration difference  $\Delta c_t$  across the channel of the thickness  $w$  between two points  $x = 0$  and  $x = w$  at the time  $t$  from the concentration difference  $\Delta c_e$  between the same points in a steady state ("equilibrium"):

$$\varepsilon = (\Delta c_e - \Delta c_t) / \Delta c_e. \quad (17)$$

Our previous conclusions<sup>13</sup> concerning the minimization of the effect of relaxation processes on the retention by optimizing the stop-flow time are, in principle, valid also for other FFF techniques and not only for colloidal particles.



As the viscosities of simple carrier liquids usually decrease with increasing temperature, the micro-TFFF carried out at elevated temperatures can be an advantage because the relaxation period could be shortened due to the increased rate of the diffusive transport phenomena of colloidal particles. Thus the temperature is an important operational parameter to be taken into account when optimizing the experimental conditions of the micro-TFFF for which the stop-flow period can make an important increase of the total time in the fractionation.

### *Cold or Hot Wall Temperature?*

The TFFF performed in standard size channels was used also for separation of colloidal particles<sup>15-24</sup>. The size of the particles, their surface properties and the interactions with the components of the carrier liquid were found as determining their retention. The effect of the cold wall temperature was studied recently in micro-TFFF of polymers which migrate towards the cold wall<sup>2</sup>. Contrary to the conclusion made by Brimhall *et al.*<sup>5</sup> that for maximum retention and selectivity the cold wall should be kept at a temperature as low as possible, we have found<sup>2</sup> that although the retention increases, the decreasing cold wall temperature has no general positive impact on the efficiency and, consequently, on the resolution. This was explained<sup>2</sup> to be a consequence of the acceleration of all transport phenomena governing and accompanying the separation and dispersion processes at higher temperatures. As a result, it does not seem that a lower cold wall temperature must be the advantageous experimental conditions in TFFF of polymers; in contrast, separation time can be substantially shortened when working at higher cold wall temperatures.

The effect of temperature was never studied in TFFF of colloidal particles. As it is an important aspect to be considered, the primary question is whether the accumulation of the fractionated colloidal particles appears at the cold or hot wall and then which temperature is decisive. According to recent experimental and theoretical findings<sup>25-28</sup>, the migration of colloidal particles towards the cold or hot wall is driven by a complex mechanism including chemical equilibria and interactions with the components of the carrier liquid. Consequently, in order to understand clearly the effect of temperature on the retention in micro-TFFF, it is imperative to know at which wall the investigated colloidal particles are concentrated due to the imposed temperature drop. In other words, it is necessary to determine whether the thermal diffusion coefficient is positive or negative.

### *Secondary Retention Mechanisms*

Whenever the temperature drop is relatively high, all particles can be compressed to the accumulation wall of the channel independently of their size and surface properties. In such a case, the mechanism of steric exclusion<sup>29</sup> dominates the separation and the elution order is from the largest to the smallest particles.

On the other hand, at high flow rates, the hydrodynamic lift forces<sup>30</sup> can play an important role and complicate the separation due to the focusing phenomenon. The mechanism of the separation can thus become quite complex. However, if the intervention of the contributing forces is mastered, both theoretically and experimentally, the micro-TFFF can offer interesting potentials to characterize various physico-chemical parameters and properties of colloidal particles.

### **EXPERIMENTAL**

#### Micro-FFF Apparatus

The apparatus for the micro-TFFF consisted of an intelligent pump model PU-980 (Jasco, Japan), an injection valve model 7410 (Rheodyne, U.S.A.) equipped with a 1  $\mu$ l loop, a UV-VIS variable wavelength intelligent detector model UV-975 (Jasco, Japan) with a measuring cell of 1  $\mu$ l, and a recorder-integrator model HP 3395 (Hewlett-Packard, U.S.A.).

The versatile micro-TFFF channel was described in detail in our previous papers<sup>1,2</sup>. Its dimensions in this study were 100  $\mu$ m  $\times$  5 mm  $\times$  100 mm. The cold wall temperature was controlled and kept constant by using a compact, low-temperature thermostat model RML 6 B (Lauda, Germany). The electric power for heating cartridge was regulated by an electronic dimmer to keep constant the temperature of the hot wall and, consequently, the temperature drop  $\Delta T$ . The temperatures of the cold and hot walls were measured by a digital thermometer (Hanna Instruments, Portugal) equipped with two thermocouples.

#### Colloidal Particles and Carrier Liquid

Polystyrene latex (PSL) particles (Duke Scientific Corp., U.S.A.) were used as model samples. Particle sizes of all studied samples are given in Table I. An aqueous solution of 0.1% of detergent Brij 78 (Fluka, Germany) and of 0.02% of NaCl was used as a carrier liquid.

### **RESULTS AND DISCUSSION**

#### *Sign of the Thermal Diffusion Coefficient*

The sign of the thermal diffusion coefficient cannot be estimated from a single value of the retention ratio. However, the magnitude of the retention ratio depends on the shape of the flow velocity profile. This means that the

difference between the retention ratio of a given species obtained under the usual conditions (with a nearly parabolic flow velocity profile formed in the carrier liquid) and the retention ratio obtained when the flow velocity profile is highly asymmetrical with respect to the central longitudinal axis of the channel can provide a relevant information on the sign of the thermal diffusion coefficient.

The flow velocity profile formed in a horizontal channel is only slightly asymmetrical due to the temperature variation of the viscosity of the carrier liquid across the channel as mentioned in Theory. A convenient, highly asymmetrical flow velocity profile is formed in thermogravitational FFF<sup>31</sup>. Whenever the fractionation channel is positioned vertically, the horizontal density gradient causes an upward convective flow at the hot wall and a downward flow at the cold wall. The coupling of this natural convective flow with the forced unidirectional flow produces an asymmetrical flow velocity profile. Its resulting shape depends on the ratio of the average velocity of the convective flow to the forced flow. An example of such a flow velocity profile is schematically shown in Fig. 1. The calculation of the forced flow velocity profile shown in Fig. 1 was performed by using an approximate but simple approach<sup>32</sup> which takes into account the temperature variation of viscosity and results in a third-degree power series. The shape of the convective flow velocity profile was calculated by using another approximate relationship<sup>33</sup>. Although this does not take into account the temperature variation across the channel and thus the temperature variation of viscosity, density and thermal expansion factor, this simplification has no importance with regard to the qualitative considerations whose goal is just the determination of the sign of the thermal diffusion coefficient. The resulting flow velocity profile in the vertical channel was calculated as the sum of two contributions by choosing arbitrarily the ratio of the average velocity of the convective flow to the forced flow. From the practical point of view, if the experimental conditions are chosen to avoid a large

TABLE I  
Particle sizes of polystyrene latexes

Polystyrene latex	Average diameter <sup>a</sup> , nm	Standard deviation <sup>b</sup> $\sigma$ , nm
PSL 60	60 $\pm$ 2.5	23
PSL 155	155 $\pm$ 4	54

<sup>a</sup> Supplier's data. <sup>b</sup> Determined by micro-TFFF.

domination of either forced or convective flow, any shape of the resulting flow velocity profile in a vertical channel is acceptable for the determination of the sign of the thermal diffusion coefficient.

It follows from Fig. 1 that the average velocity of the retained zone decreases if the forced flow has an upward direction in the vertical channel

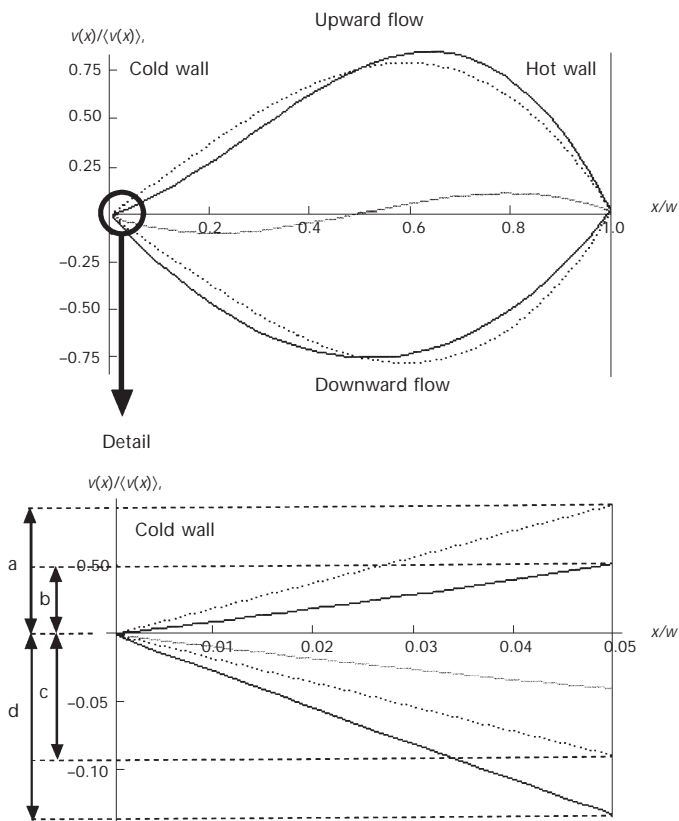


FIG. 1

Flow velocity profiles formed in horizontal and vertical channel with the upward and downward forced flow. Dotted curves correspond to non-isoviscous flow velocity profile formed in horizontal channel. Grey curve corresponds to thermal convection velocity profile formed in vertical channel (viscosity variation with temperature is neglected). Black curves correspond to flow velocity profiles resulting from the superposition of the thermal convection and either upward or downward forced flow. The negative sign on the axis of downward flow part of the ratio of the local to average flow velocity,  $v(x)/\langle v(x) \rangle$ , indicates only the downward direction of the flow but not the real values of the  $v(x)/\langle v(x) \rangle$ ; a, b and c, d distances represent the increase or decrease in the average velocity of a retained zone (for which  $\lambda = 0.05$ ) in vertical channel compared with horizontal channel

and the retained species accumulate at the cold wall compared with the average velocity in the horizontal channel (see the ratio  $a/b$  in Fig. 1), while the average velocity of a retained zone in the vertical channel increases compared with the velocity in the horizontal channel for the species accumulated at the hot wall. An increase or decrease in the velocity and, consequently, in the retention ratio is inverse with respect to the accumulation walls if the forced flow has a downward direction. However, these changes of the retention might be less important (compare the ratio  $c/d$  with  $a/b$  in detail in Fig. 1). The magnitude of the difference between the retention ratio in a vertically positioned channel and that in a horizontal channel depends on the ratio of the average velocity of the forced flow to the average velocity of the natural convection, which determines the shape of the resulting flow velocity profile.

The operational conditions of the micro-TFFF have to be carefully chosen for the experiments whose goal is to determine the sign of the thermal diffusion coefficient. The retention of the studied sample should be high enough to avoid the shift of the peak position on the fractogram due to the relaxation processes leading to a steady-state concentration distribution across the channel, which is not established immediately after the injection of the sample. Such a shift appears if the relaxation period is long compared with the whole retention time and it could obliterate the retention changes due to the asymmetry of the flow velocity profile in a vertical channel. Otherwise, it must be stressed that the micro-TFFF is well adapted to such an experiment because the small size of the channel makes no difficulties in working with the channel at any chosen position.

The fractograms of PSL 155 sample obtained in a horizontally and vertically (upward and downward flow) positioned channel under the given experimental conditions are shown in Fig. 2. There is practically no difference between the fractograms obtained in a horizontal channel and vertically positioned channel with downward forced flow. On the other hand, the change of the peak position and of the width of the fractogram in vertical channel with upward forced flow is small but well reproducible. The theoretical explanation of this observation was given in the preceding paragraph. This result indicates that the accumulation wall of the studied sample is the cold wall.

Similar experiments were carried out under different experimental conditions, namely at a lower temperature drop  $\Delta T$  and at different temperatures of the cold wall. The fractograms obtained in horizontal and vertical channel (with upward forced flow) are shown in Fig. 3. The differences in the positions of the fractogram peaks are relatively low but indicate again that

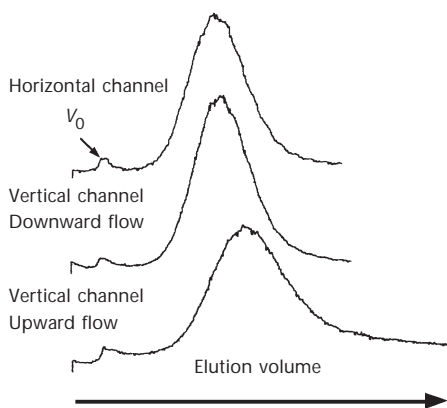


FIG. 2

Fractograms of PSL 155 sample obtained in horizontal and vertical channel with the upward (channel end up) and downward (end down) forced flow. Experimental conditions: flow rate 20  $\mu\text{l}/\text{min}$ ,  $\Delta T = 26 \text{ K}$ ,  $T_c = 309 \text{ K}$

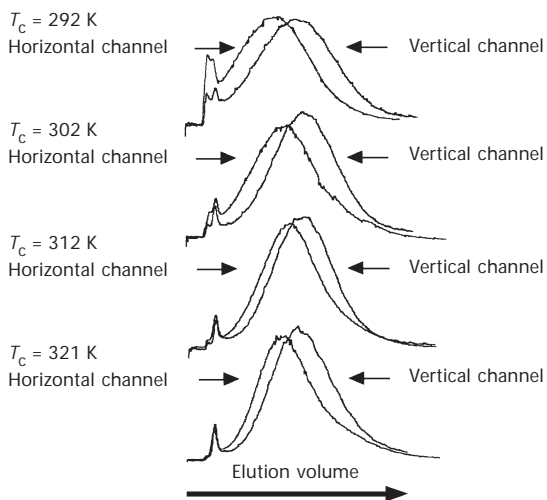


FIG. 3

Effect of the cold wall temperature on the fractograms of PSL 155 sample obtained in horizontal and vertical channel with the upward forced flow. Experimental conditions: flow rate 20  $\mu\text{l}/\text{min}$ ,  $\Delta T = 19 \text{ K}$

the sample migrates towards the cold wall. At the lowest temperature of the cold wall, the fractograms exhibit an important relaxation peak which elutes before the void volume peak. When increasing the cold wall temperature, the relaxation peak disappears progressively, the fractograms are narrower, and the maximum of the fractograms is shifted first to higher retention volumes and then to lower ones. The effect of temperature is studied and discussed in more detail later on.

The casual effect of the sedimentation of the particles due to natural gravitation was investigated by the experiments carried out in a horizontally and vertically positioned channel with upward and downward flow at  $\Delta T = 0$  K and at the same and two times lower flow rates as with the temperature drop applied. A two times lower flow rate was applied in order to have about the same elution time and casually the same sedimentation time as in the case of the retained solutes with the temperature drop applied. The retention times and the whole shapes of the fractograms in all these cases were identical and corresponded to an unretained species as can be seen in Fig. 4. This result is absolutely not surprising with regard to the size and stability of the concerned colloidal suspensions. As a result, non-detectable contribution of the sedimentation means that the observed retention ratio changes in the vertical channel compared with the horizontal channel correspond exclusively to the contribution of the natural convective flow and that the accumulation wall has been determined accurately.

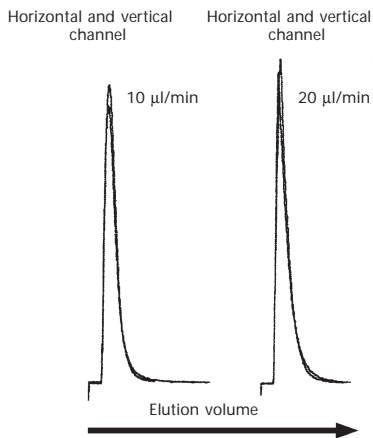


FIG. 4

Fractograms of PSL 155 sample obtained in horizontal and vertical channel with the upward and downward forced flow without application of the thermal field. Experimental conditions: flow rates 10 and 20  $\mu\text{l}/\text{min}$ ,  $\Delta T = 0$  K,  $T_c = 303$  K

### *Effect of the Temperature*

It has been found that the studied PSL samples accumulate at the cold wall under the given experimental conditions. The question, however, is which temperature has to be used in order to interpret accurately its effect on the retention. This problem was already mentioned by Brimhall *et al.*<sup>5</sup> They have chosen the temperature  $T_{cg}$  at the centre of gravity of the exponential concentration distribution across the channel of the retained species. This temperature can be calculated from<sup>5</sup>:

$$T_{cg} = T_c + f(x_{cg}, w, \Delta T, \kappa_t), \quad (18)$$

where  $T_c$  is the temperature of the cold wall,  $x_{cg}$  is the position of the center of gravity, and  $\kappa_t$  is the thermal conductivity of the carrier liquid which is dependent on temperature. The operational parameters within the brackets on the right-hand side of Eq. (18) are practically constant ( $x_{cg}$ ,  $w$ ,  $\Delta T$ ) or vary very slightly ( $\kappa_t$ ). Moreover, the  $\Delta T$  applied in the experiments was low which means that the second term on the right-hand side of Eq. (18) can reach the values of the order of tenths of kelvin and thus the use of the cold wall temperature is justified to demonstrate simply the effect of the temperature on the retention.

As a matter of fact, the course of the theoretical dependence of the retention on the temperature expressed by Eq. (13) cannot be estimated *a priori*. The problem is that the current knowledge and understanding of the thermal diffusion of colloidal particles is very limited and it is not possible to estimate whether the temperature dependence of the viscosity of the carrier liquid in Eq. (13) will dominate over the temperature dependence of the thermal diffusion coefficient or *vice versa*. All interactions and chemical equilibria mentioned in Theory are susceptible to variations from one multi-component system to the other and, consequently, to changes in dependence of retention on temperature. An enormous experimental and theoretical research is needed to fully understand the concerned phenomena. This work aims to contribute to the understanding of the behaviour of a relatively simple system.

The effect of the cold wall temperature was investigated within a broad temperature range from nearly the freezing point to the boiling point of pure water (which was the major component of the carrier liquid) and at a constant temperature drop  $\Delta T = 19$  K. Some chosen fractograms are shown in Fig. 5. The main peak of the retained PSL 155 sample is not well sepa-



rated from the relaxation and void volume peaks at the lowest cold wall temperature of 280 K. When increasing the cold wall temperature, the relaxation peak progressively disappears, the maximum of the peak corresponding to the retained sample is displaced to higher retention volumes and the resolution between the main peak and the void volume peak increases up to the 312 K. Further increase in the cold wall temperature causes the retention inversion, which decreases, but the separation of the main and void volume peaks decreases only very slightly. The selected fractograms in Fig. 5 were all obtained at the flow rate of 20  $\mu\text{l}/\text{min}$  and without the stop-flow procedure applied to reduce the effect of the relaxation phenomena.

All experimental results concerning PSL 155 and PSL 60 samples, obtained at two flow rates, 10 and 20  $\mu\text{l}/\text{min}$ , are visualized in Fig. 6, showing the variation of the retention ratio  $R$  as a function of the cold wall temperature. It can be seen in Fig. 6 that the shapes of the retention ratio  $R$  versus the cold wall temperature plots are independent of the size of the retained colloidal particles and of the flow rate under the given experimental conditions. The dependence of the retention ratio on the cold wall temperature (within the range from the minimum temperature to the temperature at which the retention ratio reaches its minimum value) can be explained by the shift of the peak position of the fractogram due to the part of the retained sample that does not reach the steady state during the initial stages

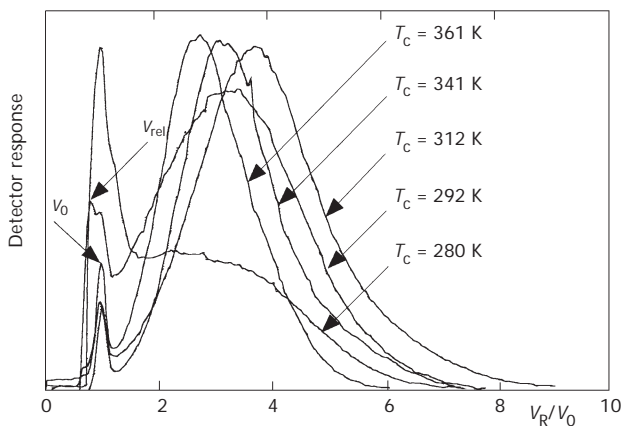


FIG. 5

Effect of the cold wall temperature within an extended temperature range on the fractograms of PSL 155 sample obtained in horizontal channel. Experimental conditions: flow rate 20  $\mu\text{l}/\text{min}$ ,  $\Delta T = 19$  K

of the separation. On the other hand, the increase in the retention ratio above its minimum value, lying approximately within the range from 300 to 310 K, with further increase in the cold wall temperature is completely different compared with the previous observations of the temperature dependence of the retention of flexible macromolecules<sup>2,4,5</sup> but it is coherent with the theoretical prediction given by Eq. (13). A simple increase in the temperature drop to  $\Delta T = 26$  K resulted in an increased retention (decreased retention ratio) of sample PSL 155 at a higher flow rate of 20  $\mu\text{l}/\text{min}$ , as shown in Fig. 6. The dependence of  $R$  versus the cold wall temperature obtained under these conditions is almost identical to that measured at a lower temperature drop of  $\Delta T = 19$  K and at a lower flow rate of 10  $\mu\text{l}/\text{min}$ . The minimum of these dependences lies approximately within the same temperature range. This result could indicate that a part of the retained particles is not yet enough relaxed after the injection even if the fractograms do not exhibit a relaxation peak (with the exception of the fractogram obtained at the lowest temperature of the cold wall).

An explicit demonstration of the contribution of the primary relaxation processes to the course of the dependence of the retention ratio on the cold wall temperature was performed by repeating the micro-TFFF of the PSL 155

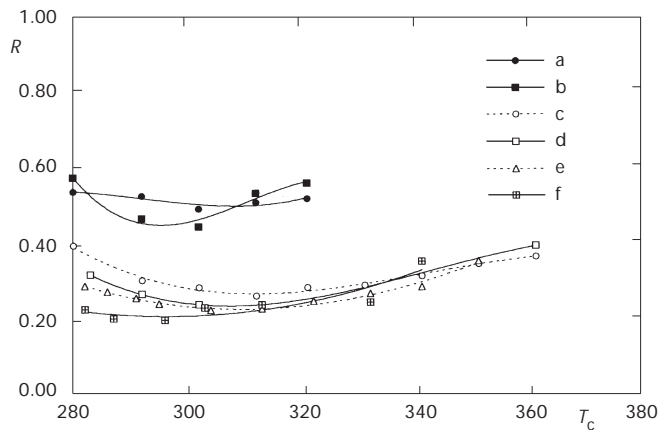


FIG. 6

Effect of the cold wall temperature within an extended temperature range on the retention ratio  $R$  of the PSL 60 and PSL 155 samples obtained in horizontal channel at two different flow rates without and with application of the stop-flow procedure. Experimental conditions: a PSL 60, 10  $\mu\text{l}/\text{min}$ ,  $\Delta T = 19$  K, without stop-flow; b PSL 60, 20  $\mu\text{l}/\text{min}$ ,  $\Delta T = 19$  K, without stop-flow; c PSL 155, 20  $\mu\text{l}/\text{min}$ ,  $\Delta T = 19$  K, without stop-flow; d PSL 155, 10  $\mu\text{l}/\text{min}$ ,  $\Delta T = 19$  K, without stop-flow; e PSL 155, 20  $\mu\text{l}/\text{min}$ ,  $\Delta T = 26$  K, without stop-flow; f PSL 155, 20  $\mu\text{l}/\text{min}$ ,  $\Delta T = 26$  K, with stop-flow

sample at a higher temperature drop of  $\Delta T = 26$  K and with the stop-flow procedure applied after the injection. The optimum stop-flow procedure was chosen according to the results of our recent detailed experimental study<sup>34</sup> of high-speed micro-TFFF. With respect to this study, the stop-flow time calculated theoretically by using the Eqs (14) to (17) is between 165 and 180 s for the species whose  $R = 0.2$  and the anticipated deviation from the steady state is between 0.5 and 2%. The experimental verification of this stop-flow time was carried out under the conditions at which a part of the particles obviously did not reach the steady state after the injection and the relaxation peak appeared in the fractogram. Although the time of the injection calculated with regard to the volume of the injection loop, the volume of the capillary connecting the injector with the channel and the flow rate during the injection was 30 s, the experimental time of the injection was also varied in order to check the optimum conditions of the injection and stop-flow procedure. The results are shown in Fig. 7. It can be seen in Fig. 7, that both the longer and shorter than 30 s injection times result in broader retained peaks. On the other hand, a longer stop-flow time of 10 min compared with the theoretically calculated optimum of 3 min has not any effect on the shape and position of the retained peak. As a result, the 30 s injection and 3 min stop-flow times were chosen for the experiments shown in Fig. 6 with the application of this injection-stop-flow procedure.

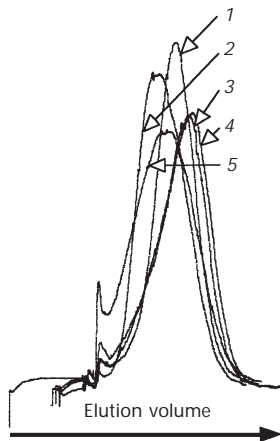


FIG. 7

Fractograms of the PSL 155 sample obtained under various conditions of the stop-flow procedure. Experimental conditions: flow rate 20  $\mu\text{l}/\text{min}$ ,  $\Delta T = 26$  K,  $T_c = 283$  K. 1 Injection 30 s, stop-flow 3 min; 2 injection 60 s, stop-flow 3 min; 3 injection 15 s, stop-flow 3 min; 4 injection 15 s, stop-flow 10 min; 5 injection 7 s, stop-flow 3 min

The results in Fig. 6 show that the retention ratio increases monotonically within almost the whole investigated temperature range in the experiments with the stop-flow procedure applied. In this case, the effect of the primary relaxation processes is substantially reduced and this explains the fact that the retention ratio *versus* the cold wall temperature dependence increases within the investigated temperature range.

As far as the casual effect of the secondary retention mechanisms mentioned in Theory is concerned, namely the mechanism of steric exclusion and the influence of the lift forces, the elution order found for an extended range of the particle sizes and within an extended range of the flow rates confirmed in our recent study<sup>34</sup> that these effects do not appear under the experimental conditions applied in this work.

The above experimental findings evoke the question whether an optimum temperature of the accumulation wall exists with regard to the analytical performance of the micro-TFFF of colloidal particles. It seems that it is advantageous to work at an elevated temperature to accelerate all transport phenomena and thus to reduce the time necessary to establish the steady-state concentration distribution of the retained species after the injection of the sample into the channel even if the stop-flow procedure is applied. Thus, the negative consequences of the relaxation phenomena can be completely suppressed. On the other hand, it is not evident whether the micro-TFFF of the colloidal particles carried out at higher temperatures could be advantageous. The analytical utility to carry out the experiments at higher temperatures can be estimated by calculating the ratio  $\sigma/V_{av}$ , where  $V_{av}$  is the average retention volume and  $\sigma$  is the standard deviation characterizing the width of the fractogram. The ratio  $\sigma/V_{av}$  provides a good estimation of the variation of the performance (resolution) of fractionation with the temperature. The  $V_{av}$  values were calculated from the experimental fractograms by using:

$$V_{av} = \frac{\sum V_i h_i}{\sum h_i}, \quad (19)$$

where  $h_i$  are the heights of the fractogram from the baseline at the corresponding retention volumes  $V_i$ . The  $\sigma$  values were calculated from:

$$\sigma = \left[ \frac{\sum (V_i - V_{av})^2 h_i}{\sum h_i} \right]^{0.5}. \quad (20)$$

The results of the calculations are given in Table II. A detailed examination of these results indicates a weak tendency of the ratio  $\sigma/V_{av}$  to decrease with increasing temperature in the experiments carried out at a lower tem-

TABLE II  
Temperature dependence of the performance of micro-TFFF

Cold wall temperature, K	Average retention volume $V_R$ arbitrary units	Standard deviation $\sigma$ arbitrary units	$\sigma/V_R$
Flow rate 20 $\mu$ l/min, $\Delta T = 19$ K, without application of the stop-flow procedure			
312	3.77	1.200	0.318
321	3.49	1.200	0.344
341	3.18	1.015	0.319
351	2.90	0.953	0.328
361	2.75	0.768	0.279
Flow rate 20 $\mu$ l/min, $\Delta T = 26$ K, without application of the stop-flow procedure			
292	3.85	1.269	0.330
294	4.08	1.108	0.272
304	4.38	0.992	0.226
313	4.31	0.885	0.205
322	4.00	0.731	0.183
332	3.72	0.711	0.191
341	3.50	0.667	0.191
351	2.83	0.542	0.191
Flow rate 20 $\mu$ l/min, $\Delta T = 26$ K, with application of the stop-flow procedure			
282	4.33	0.866	0.200
287	4.83	0.804	0.166
296	4.93	0.775	0.157
303	4.26	0.833	0.195
313	4.13	0.783	0.190
332	4.05	0.542	0.134
341	2.83	0.550	0.194

perature drop of  $\Delta T = 19$  K without application of the stop-flow procedure. A more pronounced tendency of the ratio  $\sigma/V_{av}$  to decrease with increasing temperature is exhibited in the experiments carried out at a higher temperature drop of  $\Delta T = 26$  K without the stop-flow period. Finally, the ratio  $\sigma/V_{av}$  is almost constant, independent of the temperature for the experiments performed at a higher temperature drop of  $\Delta T = 26$  K with application of the stop-flow procedure. Whenever a significant part of the particles moves along the channel far from the steady state because their transport to the accumulation wall is slower due to the lower temperature drop, a higher temperature helps only weakly to reduce the broadening and displacement of the zone by acceleration of the transport processes. The zones are broad from the very beginning of the elution and this cannot be compensated by elution at higher temperature. On the other hand, if the temperature drop is higher, the experiments carried out at higher temperatures of the accumulation wall are advantageous because the accelerated relaxation processes can help to achieve the steady state very rapidly without the need to apply the stop-flow procedure. Obviously, the most accurate results are obtained if the stop-flow procedure is applied but still, higher temperatures of the accumulation wall can have a positive impact and reduce the zone broadening. It can be concluded that the results could slightly favour the micro-TFFF performed at higher temperatures. It is, of course, necessary to take into account thermal stability of the fractionated particles.

## CONCLUSION

The effect of the accumulation wall temperature in micro-TFFF on the retention of colloidal particles suspended in an aqueous carrier liquid was studied for the first time. It has been found that the dependence of the retention ratio on temperature exhibits a minimum for moderately retained species. This behaviour can be explained by the contribution of the relaxation phenomena within the low-temperature range until the mentioned minimum and by the temperature dependence of the diffusion coefficient of the retained species at higher temperatures. This means that the transport processes that accelerate with increasing temperature lead to a more rapid establishment of the quasi-steady state from the very beginning of the fractionation. With the steady state once established at a very early stage, the opposite tendency (the increase in the retention ratio) was observed, which is probably due to the dominating temperature variation of the diffusion coefficient.

Due to the fact that the accumulation wall (cold or hot) is never *a priori* known (in lack of a satisfactory theory and experimental data), it is necessary to carry out a convenient experiment allowing to determine at which wall the retained species are concentrated. A comparison of the retention ratios obtained in a horizontal and vertical channel (with upward forced flow) under the conditions of thermogravitational FFF allows such a determination. The newly invented micro-TFFF is very convenient for these experiments because the reduced size of the channel allows to work very easily at any chosen position.

## REFERENCES

1. Janča J.: *J. Liq. Chromatogr. Relat. Tech.* **2002**, *25*, 683.
2. Janča J.: *Collect. Czech. Chem. Commun.* **2002**, *67*, 1596.
3. Janča J.: *J. Liq. Chromatogr. Relat. Tech.* **2002**, *25*, 2173.
4. Myers M. N., Caldwell K. D., Giddings J. C.: *Sep. Sci.* **1974**, *9*, 47.
5. Brimhall S. L., Myers M. N., Caldwell K. D., Giddings J. C.: *J. Polym. Sci., Polym. Phys. Ed.* **1985**, *23*, 2443.
6. Myers M. N., Chao W., Chen Ch.-I., Mumar V., Giddings J. C.: *J. Liq. Chromatogr. Relat. Tech.* **1997**, *20*, 2757.
7. Edwards T. L., Gale B. K., Frazier A. B.: *Anal. Chem.* **2002**, *74*, 1211.
8. Janča J.: *Field-Flow Fractionation: Analysis of Macromolecules and Particles*. Marcel Dekker, Inc., New York 1988.
9. Schimpf M. E., Caldwell K. D., Giddings J. C.: *Field-Flow Fractionation Handbook*. John Wiley & Sons, New York 2000.
10. Hovingh M. E., Thompson G. H., Giddings J. C.: *Anal. Chem.* **1970**, *42*, 195.
11. Giddings J. C., Chang J. P., Myers M. N., Davis J. M., Caldwell K. D.: *J. Chromatogr.* **1983**, *255*, 359.
12. van Asten A. C., Boelens H. F. M., Kok W. T., Poppe H.: *Sep. Sci. Technol.* **1994**, *29*, 513.
13. Janča J., Chmelík J., Příbylová D.: *J. Liq. Chromatogr.* **1985**, *8*, 2343.
14. Mason M., Weaver W.: *Phys. Rev.* **1924**, *23*, 412.
15. Liu G., Giddings J. C.: *Anal. Chem.* **1991**, *63*, 296.
16. Liu G., Giddings J. C.: *Chromatographia* **1992**, *34*, 483.
17. Shiundu P. M., Liu G., Giddings J. C.: *Anal. Chem.* **1995**, *67*, 2705.
18. Shiundu P. M., Giddings J. C.: *J. Chromatogr., A* **1995**, *715*, 117.
19. Ratanathanawongs S. K., Shiundu P. M., Giddings J. C.: *Colloids Surf., A* **1995**, *105*, 243.
20. Giddings J. C., Shiundu P. M., Semenov S. N.: *J. Colloid Interface Sci.* **1995**, *176*, 454.
21. Jeon S. J., Schimpf M. E.: *Polym. Mater. Sci. Eng.* **1996**, *75*, 4.
22. Van Batten C., Hoyos M., Martin M.: *Chromatographia* **1997**, *45*, 121.
23. Jeon S. J., Schimpf M. E., Nyborg A.: *Anal. Chem.* **1997**, *69*, 3442.
24. Mes E. P. C., Tijssen R., Kok W. Th.: *J. Chromatogr., A* **2001**, *907*, 201.
25. Semenov S. N.: *J. Microcolumn Sep.* **1997**, *9*, 287.
26. Semenov S. N.: *J. Liq. Chromatogr. Relat. Tech.* **1997**, *20*, 2687.
27. Lenglet J.: *Ph.D. Thesis*. University Paris 7, 1996.

28. Morozov K. I. in: *Thermal Nonequilibrium Phenomena in Fluid Mixtures* (W. Koehler and S. Wiegand, Eds), p. 1. Lecture Notes in Physics. Springer, Berlin, Heidelberg 2000.
29. Giddings J. C.: *Sep. Sci. Technol.* **1978**, 13, 241.
30. Caldwell K. D., Nguyen T. T., Myers M. N., Giddings J. C.: *Sep. Sci. Technol.* **1979**, 14, 935.
31. Giddings J. C., Martin M., Myers M. N.: *Sep. Sci. Technol.* **1979**, 14, 611.
32. Martin M., Giddings J. C.: *J. Phys. Chem.* **1981**, 85, 727.
33. Giddings J. C., Martin M., Myers M. N.: *Sep. Sci. Technol.* **1979**, 14, 611.
34. Janča J.: *J. Liq. Chromatogr. Relat. Tech.* **2003**, 26, 835.